

Current Biology, Volume 29

Supplemental Information

Infraslow State Fluctuations Govern

Spontaneous fMRI Network Dynamics

Daniel Gutierrez-Barragan, M. Albert Basson, Stefano Panzeri, and Alessandro Gozzi

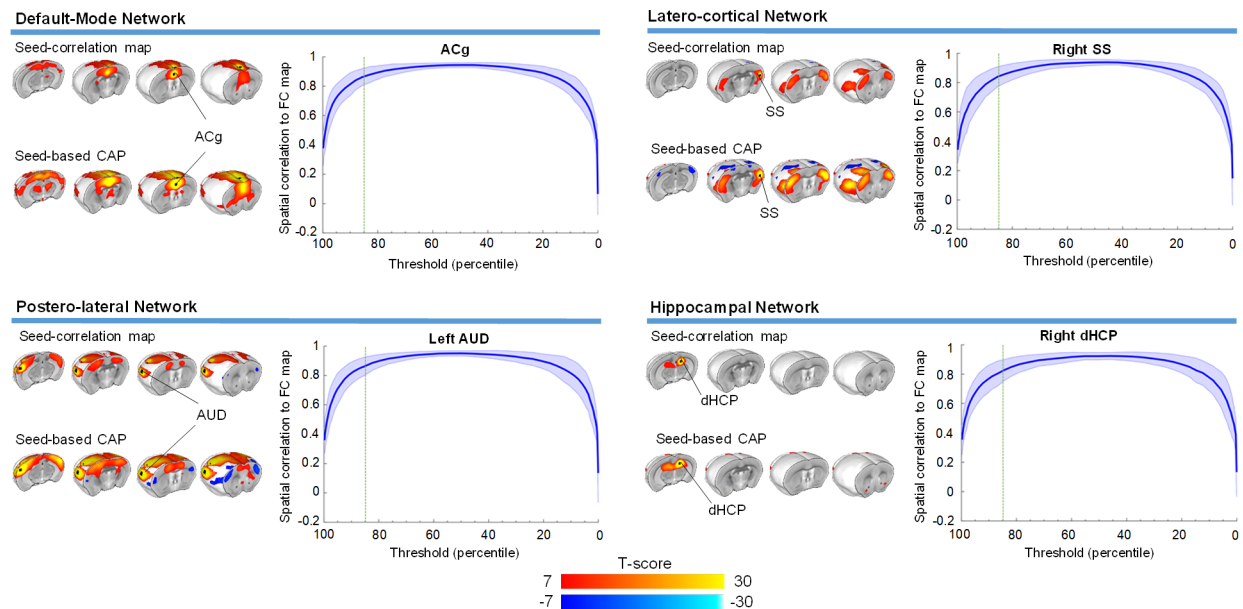


Figure S1. Selective fMRI frame averaging recapitulates rsfMRI network activity. Related to Figure 1. rsfMRI networks obtained via seed-based correlation are spatially recapitulated by averaging fMRI frames exhibiting peak regional BOLD fMRI activity (seed-based CAPs). This relationship is illustrated for four representative mouse rsfMRI networks mapped via seed-based correlation analysis (ACg, anterior cingulate, SS, somatosensory cortex, AUD, auditory cortex, dHCP, dorsal hippocampus). Plots on the right illustrate the spatial overlap between seed-based correlation maps and seed-based CAPs, as a function of the percentage of frames used for the computation of the latter (group mean \pm SEM). The dashed green line indicates the 15-percentile threshold employed for seed-based CAP visualization.

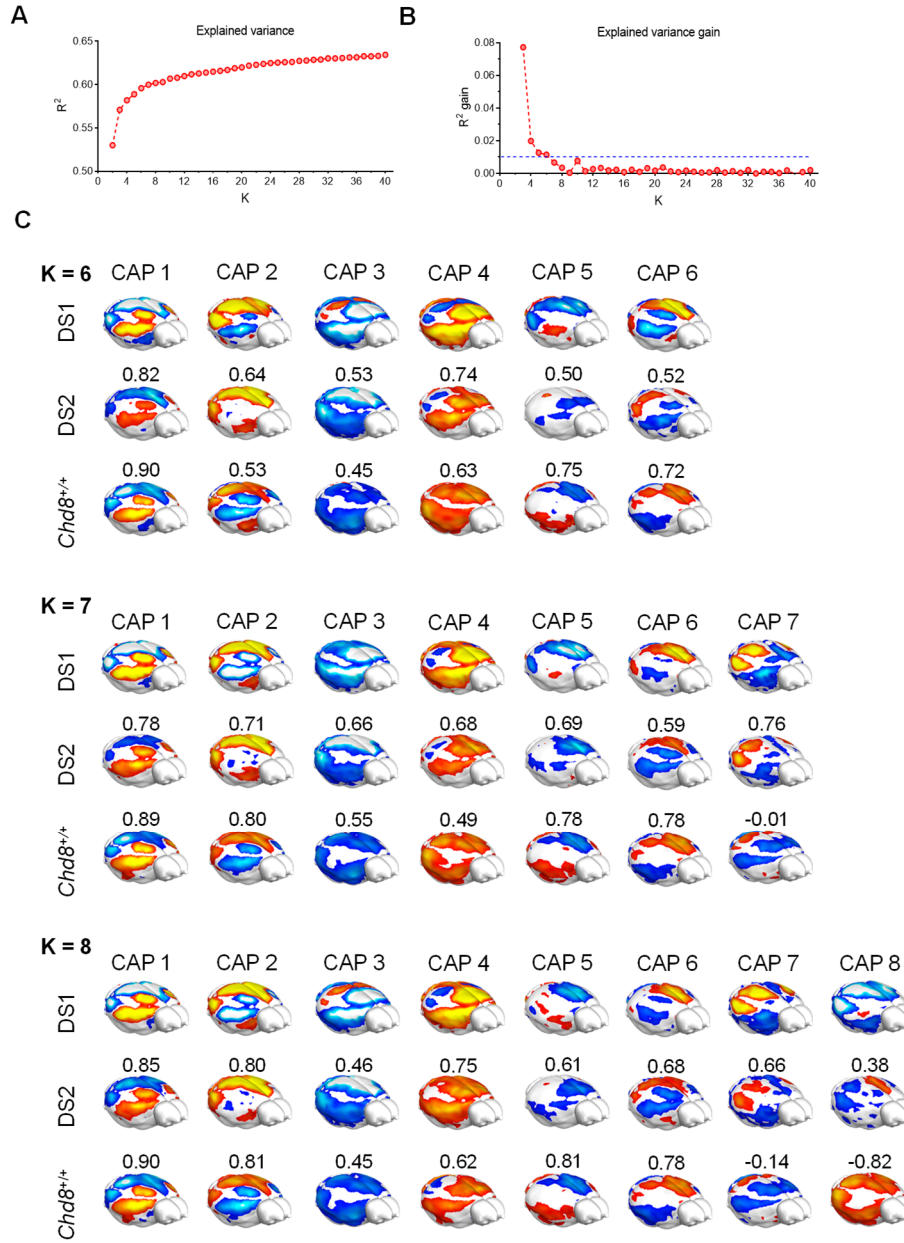


Figure S2. Selection of optimal number of clusters. Related to Figure 2. (A) Variance explained by clustering dataset 1 with $k = 2 - 40$. (B) Percentage gain in variance explained when advancing from $k-1$ to k . The dashed green line indicates 1% gain in variance explained. (C) Whole-brain representations of CAPs found with $k = 6, 7$, and 8 in dataset 1 ($n = 40$, 500 fMRI frames per subject), and their matched CAPs found in dataset 2 ($n = 41$, 300 frames per subject) or dataset 3 (CHD8^{+/+} control mice, $n = 23$, 450 frames per subject).

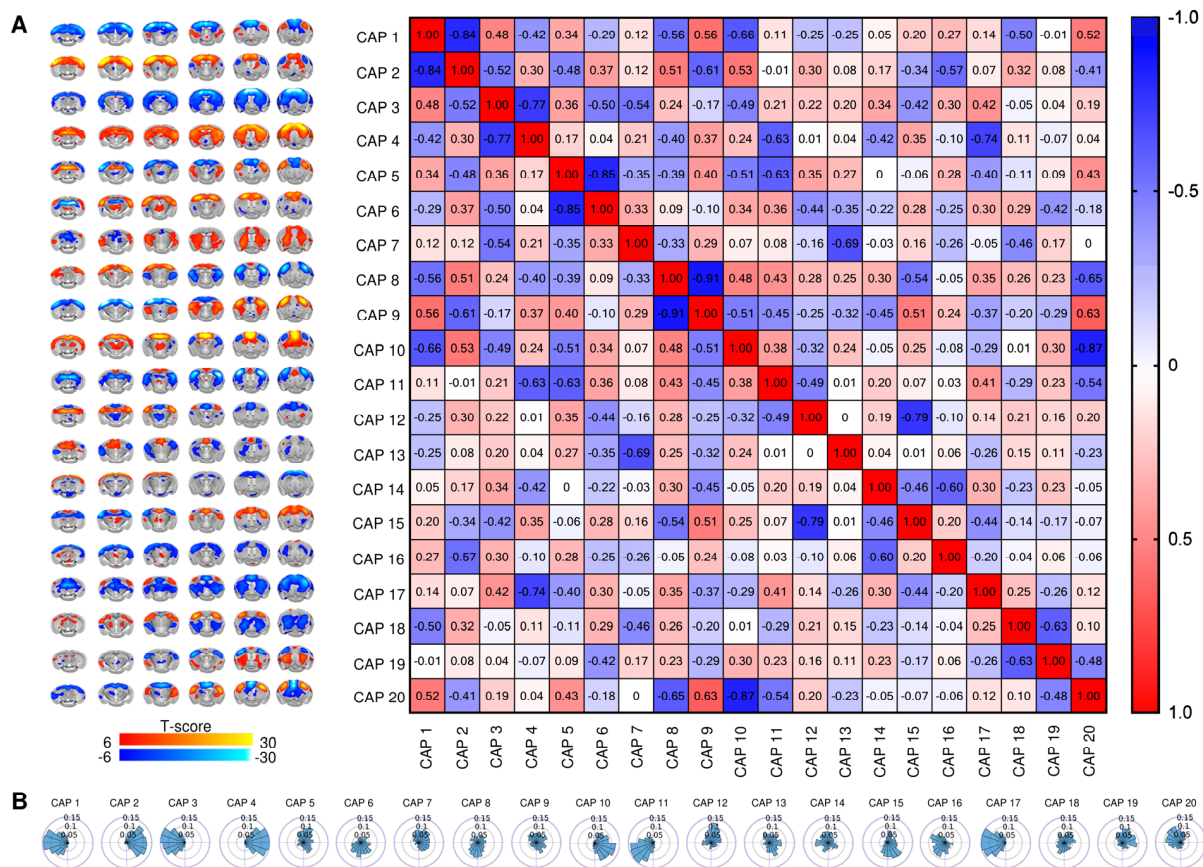


Figure S3. Functional states obtained with $k = 20$. Related to Figures 2 and 5. (A) Left - Whole brain representation of the functional brain states (CAPs) identified at the group level. Red/yellow indicates co-activation (i.e. high fMRI BOLD signal) while blue indicates co-deactivation (i.e. low fMRI BOLD signal) ($p < 0.01$, Bonferroni corrected). Right – Between CAP similarity matrix denoting the spatial correlations between the group CAP maps. (B) GS phase distribution at the occurrence of each CAP within GS cycles. Notice that CAPs 1-6 robustly maintain their spatial coverage, and GS phase distributions as with the partition with $k = 6$.

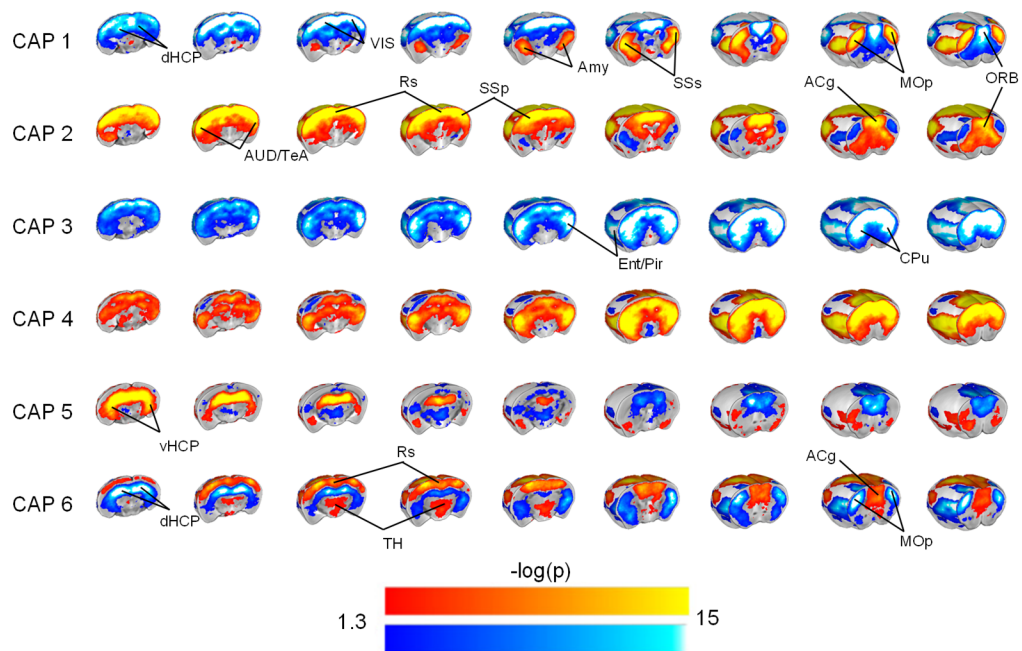


Figure S4. Subject-level voxel-wise incidence probability of CAPs. Related to Figures 2 and 3. Base ten p-values of a binomial test comparing voxel-wise incidence of subjects in each of the identified states (null, $q = 0.5$, one tailed directional test). $\text{Log}(0.05) = 1.3$.

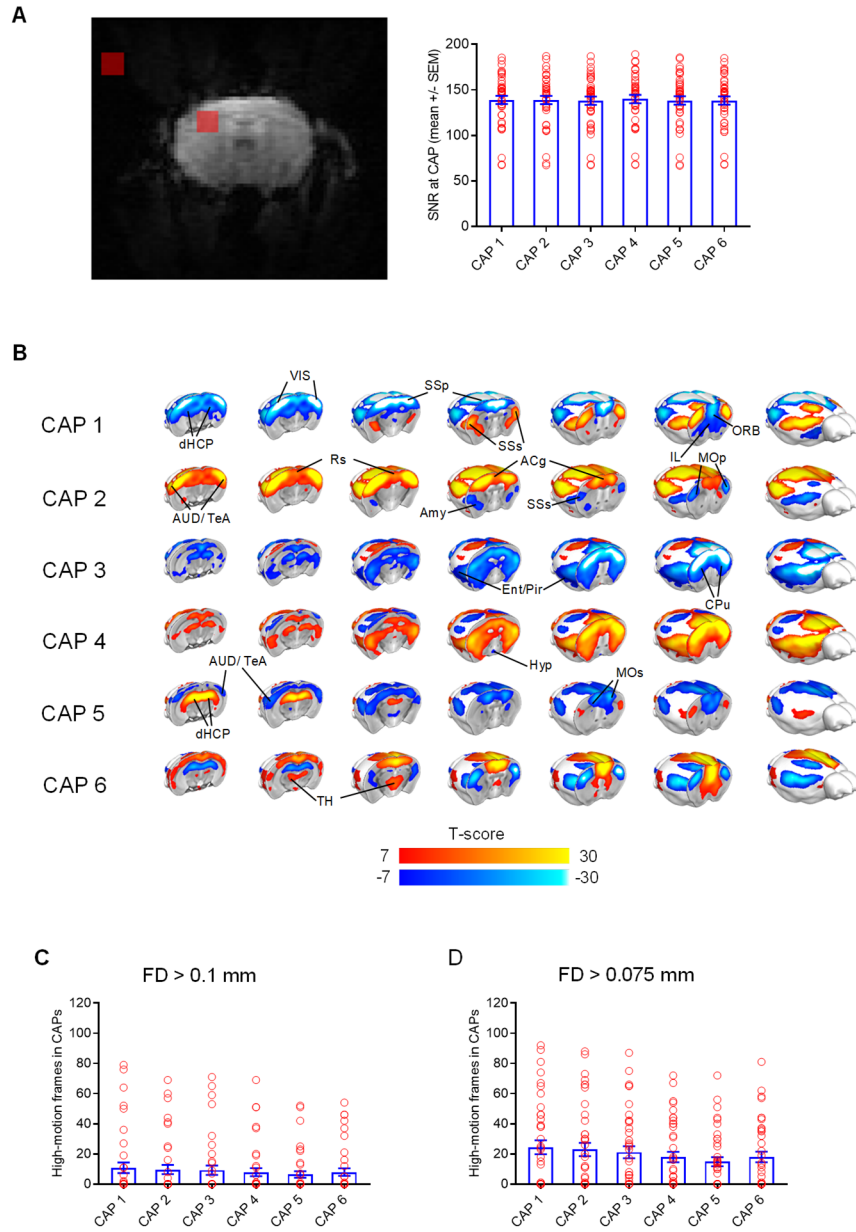


Figure S5. CAPs are not contaminated by motion or SNR fluctuations. Related to Figure 2. (A) Left – Representative raw fMRI frame showing the in-brain and out-brain ROI employed for signal-to-noise (SNR) calculation. Right – Group SNR mean of frames in a CAP, showing no difference in the SNR levels associated with the occurrence of each CAPs ($p = 0.98$, repeated measures ANOVA). (B) CAPs obtained by clustering rsfMRI frames upon censoring of putative motion-contaminated frames using a frame-wise displacement (FD) threshold of 75 μm . (C-D). Distribution of putative motion contaminated frames across CAPs at different frame-wise displacement (FD) thresholds (means \pm SEM).

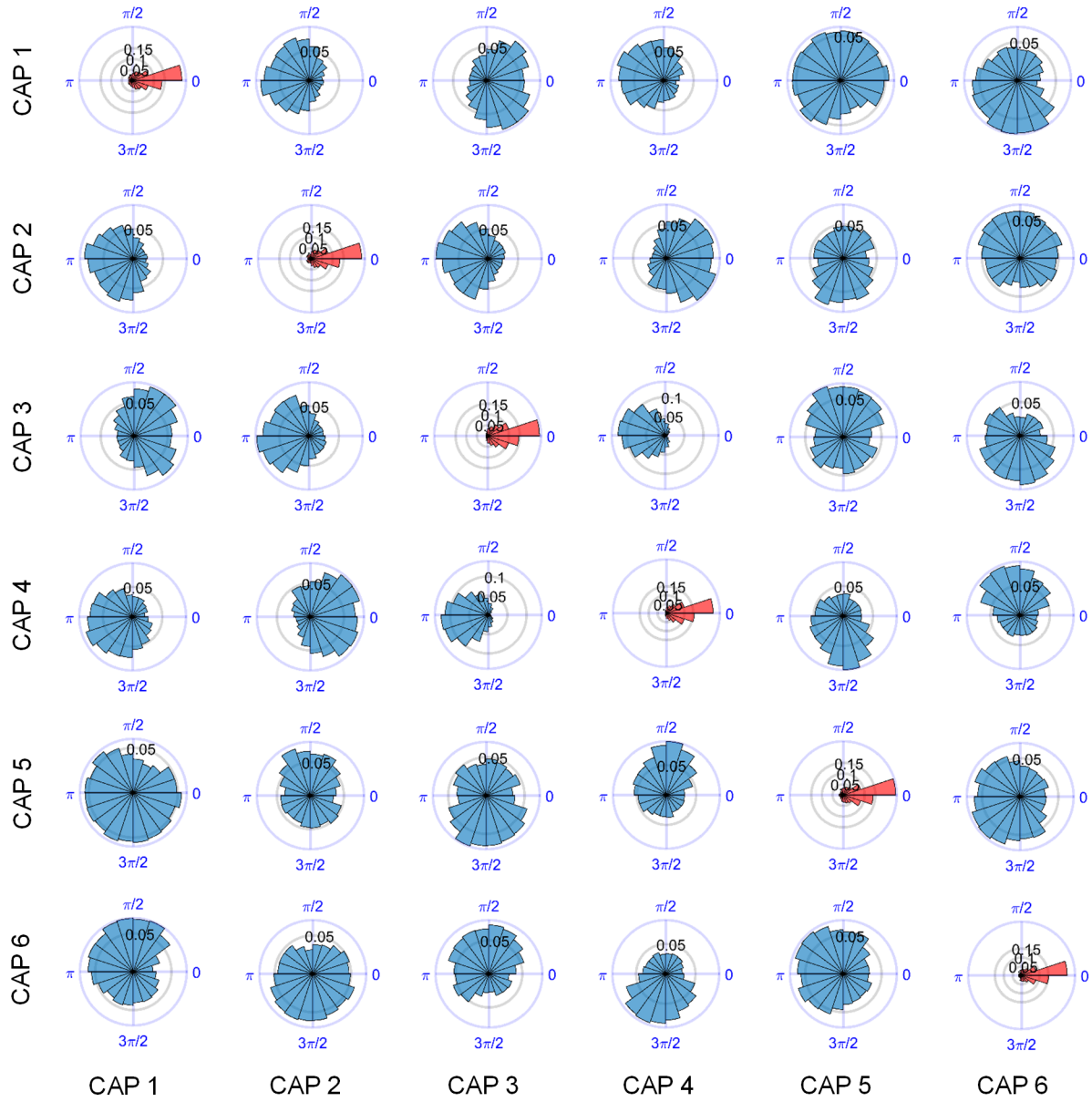


Figure S6. Functional state fluctuations are phase-coupled. Related to Figure 5. Global signal phase differences between CAP occurrences. Each panel corresponds to the circular distribution of GS phase differences between occurrences of a CAP inside a GS-cycle (rows), and the occurrences of another CAP within the same cycle and across GS cycles that were immediately adjacent in time (columns). Radial axis unit express fraction of occurrences for each CAP. All distributions significantly deviate from circular uniformity (Raleigh test, $p < 0.05$).